Extending Rotational Coherence of Interacting Polar Molecules in a Spin-Decoupled Magic Trap

Frauke Seeßelberg,[1] Xin-Yu Luo,[1,*] Ming Li,[2] Roman Bause,[1] Svetlana Kotochigova,[2] Immanuel Bloch,[1,3] and Christoph Gohle[1]

[1]*Max-Planck-Institut für Quantenoptik, 85748 Garching, Germany*
[2]*Department of Physics, Temple University, Philadelphia, Pennsylvania 19122, USA*
[3]*Fakultät für Physik, Ludwig-Maximilians-Universität München, 80799 München, Germany*

(Received 12 October 2018; published 19 December 2018)

Superpositions of rotational states in polar molecules induce strong, long-range dipolar interactions. Here we extend the rotational coherence by nearly 1 order of magnitude to 8.7(6) ms in a dilute gas of polar $^{23}Na^{40}K$ molecules in an optical trap. We demonstrate spin-decoupled magic trapping, which cancels first-order and reduces second-order differential light shifts. The latter is achieved with a dc electric field that decouples nuclear spin, rotation, and trapping light field. We observe density-dependent coherence times, which can be explained by dipolar interactions in the bulk gas.

DOI: 10.1103/PhysRevLett.121.253401

Interacting particles with long coherence times are a key ingredient for entanglement generation and quantum engineering. Cold and ultracold polar molecules [1–11] are promising systems for exploring such quantum many-body physics with long-range interactions [12,13] due to their strong and tunable electric dipole moment and long single-particle lifetime [14,15]. The manipulation of their rich internal degrees of freedom has been studied for different molecular species [16–19]. First observations include ultracold chemistry and collisions [20,21]. Nuclear spin states in the rovibronic ground state further promise exciting prospects for quantum computation due to their extremely long coherence times [22].

Rotation is a particularly appealing degree of freedom for molecules because it is directly linked to their dipolar interactions. It can be manipulated by microwave (MW) fields and superpositions of rotational states with opposite parity exhibit an oscillating dipole moment with a magnitude close to the permanent electric dipole moment d_0. Consequently, using rotating polar molecules has been proposed for quantum computation [23], to emulate exotic spin models [24] or to create topological superfluids [25].

In order to make use of the rotational transition dipole in a spatially inhomogeneous optical trap, the coupling of the rotation to the trap field needs to be canceled. To first order this may be achieved by choosing an appropriate angle between the angular momentum of the molecule and the trapping field polarization $\boldsymbol{\epsilon}$ [26] or a special trap light intensity [19] such that the differential polarizability between rotational ground and excited states is canceled. The trap is then referred to as "magic." Coherence times of about 1 ms have been achieved in bulk gases of polar molecules using these techniques [19,27]. However, this is much shorter than the dipolar interaction time, preventing observation of many-body spin dynamics.

The coherence time in such a magic trap is limited by the intensity dependence of the molecular polarizability, which originates from the coupling between rotation, nuclear spins, and the trapping light field. It has been suggested to apply large magnetic [28] or electric fields [29] to reduce these couplings and thus simplify the polarizabilities of the involved states.

In this Letter, we realize a spin-decoupled magic trap, i.e., a magic polarization angle trap with moderate dc electric fields, which simplify the hyperfine structure of the rotational transition manifold $|J = 0, m_J = 0\rangle \rightarrow |1, 0\rangle$. Here, J denotes the rotational quantum number and m_J its projection onto the electric field axis. We characterize the magic trapping condition and demonstrate how the second-order light shift is related to the electric field strength. Using Ramsey- and spin-echo interferometry, we further study the rotational coherence time of polar molecules in a spin-decoupled magic one-dimensional (1D) lattice. A coherence time of almost 10 ms is achieved for a dilute gas of ultracold $^{23}Na^{40}K$ molecules; however, we find that the coherence time decreases with increasing molecular density. Using a simple numerical model [30], we conclude that the dipolar interaction between molecules plays a dominant role in the density-dependent decoherence. This interaction can become as large as $h \times 50$ Hz, due to the large permanent dipole moment $d_0 = 2.72$ D of $^{23}Na^{40}K$ [31], at the highest accessible density of $6.8 \times 10^{10}/\mathrm{cm}^3$, comparable to the single particle dephasing.

Our experiments begin with the preparation of ultracold $^{23}Na^{40}K$ molecules in the rovibronic ground state at 300 nK [9] in several layers of a 1D lattice; see Fig. 1(a). The lattice

 © 2018 American Physical Society

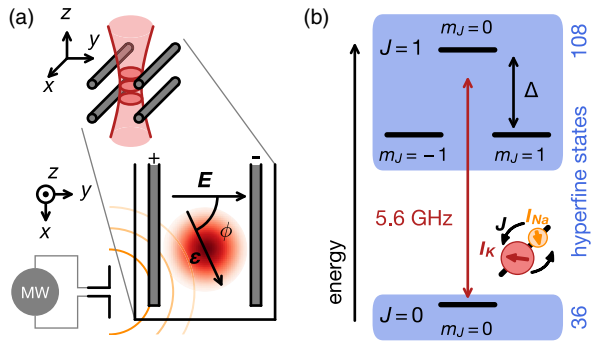

FIG. 1. (a) Schematic of the experimental setup. Molecules are confined to several pancake shaped optical traps (red) in the x-y plane, formed by a 1D optical lattice along the z axis with polarization vector $\boldsymbol{\varepsilon}$. Four in-vacuum rod electrodes (gray bars) generate dc electric fields along the y axis. The angle ϕ between $\boldsymbol{\varepsilon}$ and $\boldsymbol{E}$ can be used to adjust the first-order differential ac Stark shift between rotational states. A near-field dipole antenna emits 5.6 GHz microwaves (MWs) and couples the rotational states $|J, m_J\rangle$ (black lines) shown in (b). Blue boxes: nuclear spin states couple to rotation and mix in the $J = 1$ manifold. A dc Stark shift Δ splits the $|1, 0\rangle$ and $|1, \pm 1\rangle$ states.

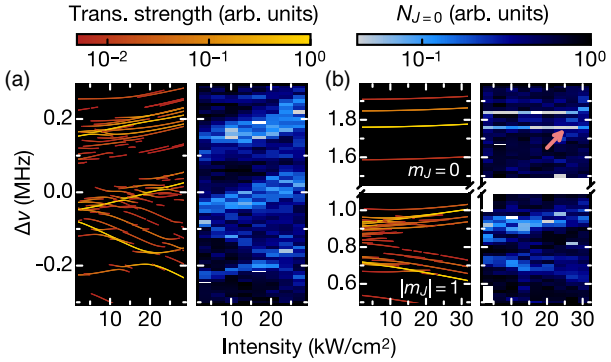

FIG. 2. The ac Stark maps of the $J = 0$ to $J = 1$ transition manifold for two electric field strengths. (a) $E = 8.8$ V/cm. Left panel: transition frequencies from the $|\downarrow\rangle$ state to the $J = 1$ manifold as a function of light intensity. The normalized transition strengths are encoded by line color. Only transitions stronger than 0.5% are shown. Right panel: molecule loss spectroscopy. Molecules remaining in $|\downarrow\rangle$ after a MW sweep are recorded (blue). (b) $E = 101.3$ V/cm at magic trapping conditions. The $m_J = 0$ component (upper panel) is separated from the $m_J = \pm 1$ components (lower panel) by the dc Stark shift Δ. Consequently, the hyperfine structure of the $m_J = 0$ manifold is simplified to two strong lines. Their transition frequency is almost independent of intensity. The red arrow denotes the $|\uparrow\rangle$ state that will be used in the following. Theoretical (experimental) data in both subfigures are normalized to the same maximum transition strength (detected atom number).

is generated by a single, linearly polarized 1550 nm retro-reflected laser beam that propagates along the z axis, which is also the direction of an 86 G magnetic field required for the molecule production. The polarization of the lattice beam can be adjusted with a half-wave plate within an uncertainty of 0.5 degrees. Initially, the molecules are prepared in the $|J, m_J, m_{I,\mathrm{Na}}, m_{I,\mathrm{K}}\rangle = |0, 0, -1/2, -4\rangle$ hyperfine state which will be referred to as the ground state $|\downarrow\rangle$. Here, m_I denotes the projections of the nuclear spins $I_{\mathrm{Na}} = 3/2$ [32] and $I_{\mathrm{K}} = 4$ [33] onto the electric field axis. A dc electric field along the y axis is generated by applying voltages to four in-vacuum rod electrodes. Eight additional auxiliary electrodes compensate residual electric field gradients to below 0.5 V/cm^2 [see the Supplemental Material [34]].

As shown in Fig. 1(b), molecules in the $J = 0$ manifold can be coupled to the first excited rotational manifold $|1, (0, \pm 1)\rangle$ via MW radiation with a frequency of $2B_{\mathrm{rot}}/h \approx 5.6$ GHz [17], B_{rot} denotes the rotational constant. There are $(2I_{\mathrm{Na}} + 1)(2I_{\mathrm{K}} + 1) = 36$ hyperfine states in the $J = 0$ manifold and 108 hyperfine states in the $J = 1$ manifold. The nuclear spins in the $J = 1$ manifold couple to rotation predominantly via the nuclear electric quadrupole moment. Furthermore, the trapping light field couples different m_J states [19,40]. Subsequently, the hyperfine levels in the excited states are mixed and their energies show many avoided crossings as a function of light field intensity; see the left panel of Fig. 2(a). Because of the strong mixing of the hyperfine levels, transition bands emerge rather than transition lines. Even when the first-order differential light shift is canceled [19,26], rotational states can therefore still rapidly dephase in an inhomogeneous optical trap. The right panel shows the result of the corresponding MW loss spectroscopy.

In order to couple to states with different transition strengths, while maintaining good spectral resolution, we sweep the MW frequency across 10 kHz in 1.15 ms. The Rabi frequency for the strongest transition is 4.0 kHz. Whenever a reduction in $|\downarrow\rangle$ molecules is detected, a transition to $J = 1$ has occurred [see the Supplemental Material [34]].

In the presence of an electric field $E = 101.3$ V/cm [see Fig. 2(b)], the $m_J = 0$ states separate from the nearly degenerate $m_J = \pm 1$ states due to the dc Stark splitting. Because this splitting is larger than all other interactions for electric fields as low as 60 V/cm, the nuclear spins decouple from the rotation, thus simplifying the ac Stark map. In addition, the rotation is decoupled from the light field, thereby reducing the curvature of the transition frequencies of these states. Simultaneously, the polarization of the lattice beam is set to the magic angle with respect to the static field $\boldsymbol{E}$, thereby realizing a spin-decoupled magic trap.

In the following, we focus on $|\uparrow\rangle$, the hyperfine state of $J = 1$, $m_J = 0$ with the largest transition strength. The dependence of the transition frequency ν on the light intensity I, the polarization angle ϕ, and the electric field E can be approximated by

$$\Delta\nu = \nu - \nu_0 = \frac{1}{h}[\Delta\alpha(\phi)I + \beta(E, \phi)I^2 + \mathcal{O}(I^3)], \quad (1)$$

where ν_0 denotes the transition frequency at $I = 0$, $\Delta\alpha = \alpha_{|\downarrow\rangle} - \alpha_{|\uparrow\rangle}$ is the differential polarizability, and β is the

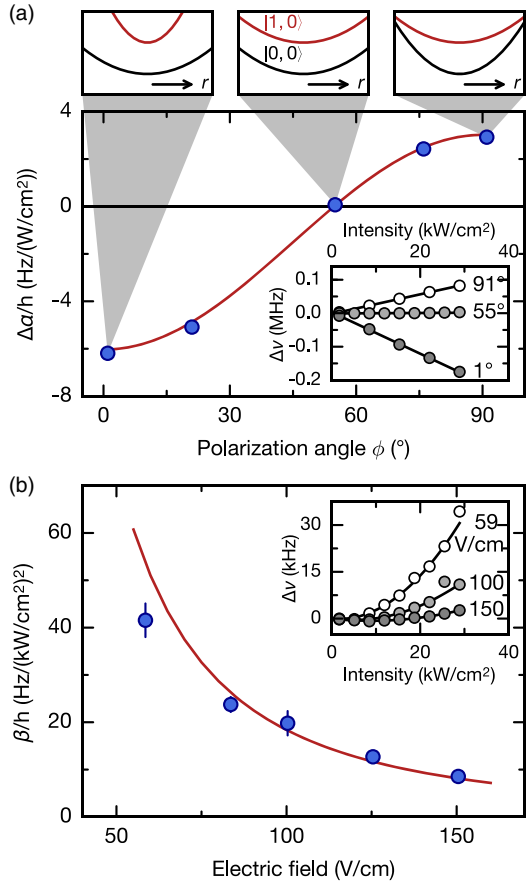

FIG. 3. Spin-decoupled magic trap. Blue circles are measurements, red lines are theory, black lines are fits of the data to Eq. (1). (a) Differential polarizability $\Delta\alpha$ for various lattice polarization angles at $E = 144.3$ V/cm. Inset: exemplary ac Stark data to extract $\Delta\alpha$. Top panels: schematics of trapping potentials of $|\downarrow\rangle$ (black lines) or $|\uparrow\rangle$ (red lines), which depend on the polarization angle ϕ. At approximately 54°, a magic trapping condition is fulfilled. (b) Hyperpolarizability β at the magic angle for various dc electric fields. Inset: exemplary ac Stark data to extract β for three electric fields. All error bars were calculated from the covariance matrix of the fits.

hyperpolarizability of $J = 1$ as $\beta \approx 0$ for $J = 0$. Specifically, $\Delta\alpha(\phi) = 2/15 \times (1 - 3\cos^2\phi)\Delta\alpha_{\mathrm{ele}}$, where $\Delta\alpha_{\mathrm{ele}} = h \times 22$ Hz/(W/cm^2) [27,34]. To characterize the magic angle for this transition, we work at $E = 144.3$ V/cm and use a π pulse for the MW spectroscopy; see Fig. 3(a). For each ϕ we measure the transition frequency ν as a function of trap intensity and find differential polarizabilities that agree well with theory. The magic condition $\Delta\alpha = 0$ occurs for $\phi = 54.0(5)°$.

To determine β, the same π-pulse spectroscopy, albeit with higher frequency resolution, is employed at $\phi = 54°$, and for various electric fields, see the inset of Fig. 3(b). We extract β (blue circles) by fitting Eq. (1) to our data and find that it decreases with increasing E. If $d_0 E \ll B_{\mathrm{rot}}$ and $d_0^2 E^2/B_{\mathrm{rot}}$ is much larger than $\Delta\alpha_{\mathrm{ele}} I$ and the Zeeman splitting of m_J states with the same hyperfine character at $E = 0$, and away from any spectral crossings, β can be derived from second-order perturbation of the energy as

$$\beta(E,\phi) = \frac{4}{15}\sin^2(2\phi)\frac{\Delta\alpha_{\mathrm{ele}}^2 B_{\mathrm{rot}}}{d_0^2 E^2}, \tag{2}$$

shown as red line in Fig. 3(b) for our parameters.

Next, we study the rotational coherence in the spin-decoupled magic trap; see Fig. 4. We use Ramsey and spin-echo pulse sequences [41] and work at $I = 3.4$ kW/cm^2. We set $E = 68.3$ V/cm, which is large enough to decouple the $|\uparrow\rangle$ state and small enough to minimize inhomogeneous broadening or temporal noise of the dc Stark shift. The MW frequency ν is set to resonance. We scan the relative phase $\Delta\theta$ between the first and second $\pi/2$ pulse at a fixed evolution time t to obtain Ramsey interference fringes. Each fringe is described by

$$N_{|\downarrow\rangle}(\Delta\theta, t) = \frac{N_{\mathrm{tot}}(t)}{2}[1 - c(t)\cos(\Delta\theta + \theta_0)], \tag{3}$$

where $c(t)$ is the measured contrast, $N_{\mathrm{tot}} = N_{|\downarrow\rangle} + N_{|\uparrow\rangle}$ is the total molecule number, and θ_0 is a phase offset due to small detunings of the MW, e.g., due to electric field changes. We measure $c(t)$ for various molecule numbers [see Fig. 4(a)] and fit a Gaussian to extract the coherence time. Because c is strictly positive in the fringe fitting, it biases the coherence time when the fringe amplitude becomes comparable to molecule number fluctuations. We therefore estimate the bias Δc for each data point individually and exclude data taken after the first point where $c < 1.5\Delta c$ [see the Supplemental Material [34]]. The Ramsey coherence time τ_c, here defined as the $1/e$ time of the fit, amounts to 8.7(6) ms for a low molecule number $N_{\mathrm{tot}} = 740(70)$, which is six times larger than previously achieved coherence times [19,27].

Residual single particle dephasing could arise due to residual differential light shifts, electric field gradients, and shot-to-shot fluctuations of the electric field. By adding a π pulse in the middle of the evolution, we obtain a spin-echo sequence that cancels the slowly varying contributions to the single particle dephasing and allows us to increase the coherence time to $\tau_c = 13(2)$ ms for low initial molecule numbers. Note that the molecules in this work are moving with the trapping period of $T_{\mathrm{trap}} = 16$ ms in the horizontal planes, which are weakly confined by the 1D lattice. Spin echo fails to suppress or even enhances the single particle dephasing when the evolution time is close to the trapping period [42]. This explains why the maximum coherence time observed in our experiment remains below T_{trap}.

Furthermore, we find that the coherence time depends on the initial molecule number and thus on density; see Fig. 4(b) [see the Supplemental Material [34]]. There could be several reasons for this, e.g., a loss of molecules. We measure an intrastate inelastic collision rate of below 3 Hz,

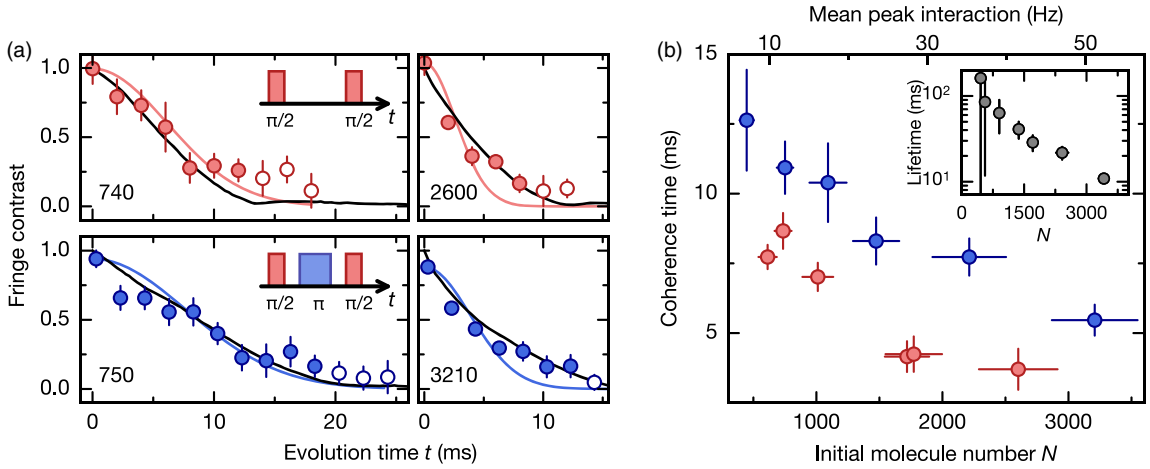

FIG. 4. Rotational coherence in the spin-decoupled magic trap. (a) Contrast of the Ramsey (red circles) and spin-echo (blue circles) fringes for various evolution times t. MW pulse sequences are shown in the upper right, initial molecular numbers in the lower left corner. Data points below the bias cutoff (empty circles) are excluded for extracting the coherence time with a Gaussian fit (colored lines). MACE simulations (black lines) of a dipolar Hamiltonian with a dephasing rate of $h \times 21(2)$ Hz [$h \times 35(2)$ Hz] describe our observations for the Ramsey (spin-echo) experiments well. (b) Ramsey (red) and spin-echo (blue) coherence times at various molecular densities. The mean dipolar interaction strength at the center of the cloud is indicated on the secondary x axis [see the Supplemental Material [34]]. The coherence time is not limited by the $1/e$ lifetime of the rotational superposition, shown in the inset. All error bars are calculated from the covariance matrix of the fits and denote 1 standard deviation.

because these collisions are suppressed by the p-wave barrier. Thus, interstate inelastic collisions dominate, which leads to equal loss of $|\downarrow\rangle$ and $|\uparrow\rangle$ and does not reduce the fringe contrast. Furthermore, this two-body loss occurs on much longer time scales than the decoherence; see inset of Fig. 4(b). Another reason for the density dependent decoherence is the strong dipolar interaction present in the system.

To qualitatively understand the decoherence of the molecular rotation caused by dipolar interactions, we use the moving average cluster expansion (MACE) method [30] to simulate the spin dynamics of randomly distributed molecules in bulk during the Ramsey or spin-echo interferometry [see the Supplemental Material [34]]. Neglecting loss and molecular motion, the system can be described by the following Hamiltonian

$$H = \sum_{i>j} \frac{U_{ij}}{2} (\hat{S}_i^+ \hat{S}_j^- + \text{H.c.}) + \sum_i \Delta(\boldsymbol{r}_i) \hat{S}_i^z, \qquad (4)$$

where the first term describes the dipolar spin-exchange interaction, where $\hat{S}_i^{\pm}$ and $\hat{S}_i^z$ are the spin-1/2 angular momentum operators of molecule i in position $\boldsymbol{r}_i$, $U_{ij} = 2d_{\uparrow\downarrow}^2/(4\pi\varepsilon_0) \times (1 - 3\cos^2\Theta_{ij})/(|\boldsymbol{r}_i - \boldsymbol{r}_j|^3)$ is the dipole-dipole interaction strength between molecules i and j, $d_{\uparrow\downarrow} = \sqrt{1/3} d_0$ is the transition dipole moment between $|\downarrow\rangle$ and $|\uparrow\rangle$ [43,44], ε_0 is the vacuum permittivity, and Θ_{ij} is the angle between the vector connecting molecules i and j and the quantization axis. The second term describes the coupling to external fields, where $\Delta(\boldsymbol{r}_i)$ is a spatially dependent detuning of the microwave transition [34]. We use $\Delta(\boldsymbol{r}_i)$ to emulate the effects of single particle dephasing, especially the uncanceled, movement-induced, time-dependent gradient in the spin-echo case. By modeling this inhomogeneity as an effective external field gradient, the Ramsey (spin-echo) signal with very low molecule number, for which the dipolar interactions can be neglected, can be reproduced. The corresponding single particle dephasing rate is $h \times 35(2)$ Hz [$h \times 21(2)$ Hz], which corresponds to a dephasing time of 9 (15) ms for the Ramsey (spin-echo) case. Using these values as input for the MACE model leads to simulation results that are consistent with experimental observations for all other densities [black lines, see the Supplemental Material [34] for all data sets], four of which are shown in Fig. 4(a). This indicates that dipolar interactions are the dominant source of the density-dependent decoherence. A theoretical model tailored to the trap geometry discussed in this Letter could improve the understanding of how molecular loss, motion, and contact interaction modify the spin dynamics in a bulk gas of polar molecules.

In conclusion, we presented a novel trapping technique for rotating molecules that cancels differential polarizability and reduces the hyperpolarizability. With this method, applicable to a broad range of polar molecules, a density dependence of the rotational coherence time is observed, which is attributed to molecular dipole-dipole interactions and characterized using a simple numerical model. For low density, coherence times as large as 13(2) ms were obtained in the molecular clouds. This opens up exciting possibilities for further experiments. The interplay between the kinetic energy and dipolar interaction could be studied in a bulk

gas of molecules. If even longer coherence times are required, a spin-decoupled magic 3D optical lattice could be used to freeze out any molecular motion. This seems very promising because rotational coherence times of about 100 ms were already achieved in a nonspin-decoupled magic 3D lattice [15]. For a near unity filling $^{23}Na^{40}K$ gas in a 3D optical lattice, we expect a dipolar interaction energy on the order of $h \times 1$ kHz, much stronger than the single particle dephasing. This will allow the observation of new states of dipolar quantum matter, e.g., a condensate of rotational excitations [45].

We thank Kaden Hazzard, Tao Shi, Gang-Qin Liu, and Richard Schmidt for inspiring discussions, Jun Ye for help with the high-precision high-voltage source, Marcel Duda and Scott Eustice for careful reading of the manuscript, and Nikolaus Buchheim and Zhen-Kai Lu for their contributions to the experimental setup. The MPQ team gratefully acknowledges support from the DFG (Grant No. FOR 2247) and the EU (UQUAM). Work at Temple University is supported by the ARO-MURI Grant No. W911NF-14-1-0378, the ARO Grant No. W911NF-17-1-0563, the AFOSR Grant No. FA9550-14-1-0321, and the NSF Grant No. PHY-1619788.

*xinyu.luo@mpq.mpg.de

[1] K.-K. Ni, S. Ospelkaus, M. De Miranda, A. Pe'er, B. Neyenhuis, J. Zirbel, S. Kotochigova, P. Julienne, D. Jin, and J. Ye, Science **322**, 231 (2008).
[2] E. S. Shuman, J. F. Barry, and D. DeMille, Nature (London) **467**, 820 (2010).
[3] T. Takekoshi, L. Reichsöllner, A. Schindewolf, J. M. Hutson, C. R. Le Sueur, O. Dulieu, F. Ferlaino, R. Grimm, and H.-C. Nägerl, Phys. Rev. Lett. **113**, 205301 (2014).
[4] P. K. Molony, P. D. Gregory, Z. Ji, B. Lu, M. P. Köppinger, C. R. Le Sueur, C. L. Blackley, J. M. Hutson, and S. L. Cornish, Phys. Rev. Lett. **113**, 255301 (2014).
[5] J. W. Park, S. A. Will, and M. W. Zwierlein, Phys. Rev. Lett. **114**, 205302 (2015).
[6] M. Guo, B. Zhu, B. Lu, X. Ye, F. Wang, R. Vexiau, N. Bouloufa-Maafa, G. Quéméner, O. Dulieu, and D. Wang, Phys. Rev. Lett. **116**, 205303 (2016).
[7] A. Prehn, M. Ibrügger, R. Glöckner, G. Rempe, and M. Zeppenfeld, Phys. Rev. Lett. **116**, 063005 (2016).
[8] T. M. Rvachov, H. Son, A. T. Sommer, S. Ebadi, J. J. Park, M. W. Zwierlein, W. Ketterle, and A. O. Jamison, Phys. Rev. Lett. **119**, 143001 (2017).
[9] F. Seeßelberg, N. Buchheim, Z.-K. Lu, T. Schneider, X.-Y. Luo, E. Tiemann, I. Bloch, and C. Gohle, Phys. Rev. A **97**, 013405 (2018).
[10] L. Anderegg, B. L. Augenbraun, Y. Bao, S. Burchesky, L. W. Cheuk, W. Ketterle, and J. M. Doyle, Nat. Phys. **14**, 890 (2018).
[11] A. L. Collopy, S. Ding, Y. Wu, I. A. Finneran, L. Anderegg, B. L. Augenbraun, J. M. Doyle, and J. Ye, Phys. Rev. Lett. **121**, 213201 (2018).
[12] S. A. Moses, J. P. Covey, M. T. Miecnikowski, D. S. Jin, and J. Ye, Nat. Phys. **13**, 13 (2017).
[13] L. De Marco, G. Valtolina, K. Matsuda, W. G. Tobias, J. P. Covey, and J. Ye, arXiv:1808.00028.
[14] A. Chotia, B. Neyenhuis, S. A. Moses, B. Yan, J. P. Covey, M. Foss-Feig, A. M. Rey, D. S. Jin, and J. Ye, Phys. Rev. Lett. **108**, 080405 (2012).
[15] B. Yan, S. A. Moses, B. Gadway, J. P. Covey, K. R. A. Hazzard, A. M. Rey, D. S. Jin, and J. Ye, Nature (London) **501**, 521 (2013).
[16] S. Ospelkaus, K.-K. Ni, G. Quéméner, B. Neyenhuis, D. Wang, M. H. G. de Miranda, J. L. Bohn, J. Ye, and D. S. Jin, Phys. Rev. Lett. **104**, 030402 (2010).
[17] S. A. Will, J. W. Park, Z. Z. Yan, H. Loh, and M. W. Zwierlein, Phys. Rev. Lett. **116**, 225306 (2016).
[18] M. Guo, X. Ye, J. He, G. Quéméner, and D. Wang, Phys. Rev. A **97**, 020501 (2018).
[19] J. A. Blackmore *et al.*, Quantum Sci. Technol. **4**, 014010 (2018).
[20] K.-K. Ni, S. Ospelkaus, D. Wang, G. Quéméner, B. Neyenhuis, M. De Miranda, J. Bohn, J. Ye, and D. Jin, Nature (London) **464**, 1324 (2010).
[21] X. Ye, M. Guo, M. L. González-Martínez, G. Quéméner, and D. Wang, Sci. Adv. **4**, eaaq0083 (2018).
[22] J. W. Park, Z. Z. Yan, H. Loh, S. A. Will, and M. W. Zwierlein, Science **357**, 372 (2017).
[23] D. DeMille, Phys. Rev. Lett. **88**, 067901 (2002).
[24] D. Peter, S. Müller, S. Wessel, and H. P. Büchler, Phys. Rev. Lett. **109**, 025303 (2012).
[25] N. Y. Yao, A. V. Gorshkov, C. R. Laumann, A. M. Läuchli, J. Ye, and M. D. Lukin, Phys. Rev. Lett. **110**, 185302 (2013).
[26] S. Kotochigova and D. DeMille, Phys. Rev. A **82**, 063421 (2010).
[27] B. Neyenhuis, B. Yan, S. A. Moses, J. P. Covey, A. Chotia, A. Petrov, S. Kotochigova, J. Ye, and D. S. Jin, Phys. Rev. Lett. **109**, 230403 (2012).
[28] Y. Deng and S. Yi, Phys. Rev. A **92**, 033624 (2015).
[29] M. Li, A. Petrov, C. Makrides, E. Tiesinga, and S. Kotochigova, Phys. Rev. A **95**, 063422 (2017).
[30] K. R. A. Hazzard, B. Gadway, M. Foss-Feig, B. Yan, S. A. Moses, J. P. Covey, N. Y. Yao, M. D. Lukin, J. Ye, D. S. Jin, and A. M. Rey, Phys. Rev. Lett. **113**, 195302 (2014).
[31] A. Gerdes, O. Dulieu, H. Knöckel, and E. Tiemann, Eur. Phys. J. D **65**, 105 (2011).
[32] D. A. Steck, *Sodium D Line Data* (2010), http://steck.us/alkalidata/sodiumnumbers.pdf.
[33] T. G. Tiecke, *Properties of Potassium* (2011), http://www.tobiastiecke.nl/archive/PotassiumProperties.pdf.
[34] See Supplemental Material at http://link.aps.org/supplemental/10.1103/PhysRevLett.121.253401 for a discussion of lattice calibration, electric field setup, ac Stark map, fitting bias of the contrast measurements, the MACE simulation, and estimations of the dipolar interaction and the single particle dephasing, which includes Refs. [35–39].
[35] S. Friebel, C. D'Andrea, J. Walz, M. Weitz, and T. W. Hänsch, Phys. Rev. A **57**, R20 (1998).
[36] R. Grimm, M. Weidemüller, and Y. B. Ovchinnikov, in *Advances In Atomic, Molecular, and Optical Physics* (Academic Press, 2000), Vol. 42, pp. 95–170, doi: 10.1016/S1049-250X(08)60186-X.

[37] P. Händel, Measurement **43**, 766 (2010).
[38] J. Shaw, *External Electric Fields: A New Tool for Controlling Ultracold Polar Molecules* (2015), https://scholar.colorado.edu/cgi/viewcontent.cgi?article=2136&context=honr_theses.
[39] H.-W. Li, S. Kar, and P. Jiang, Int. J. Quantum Chem. **113**, 1493 (2013).
[40] P. D. Gregory, J. A. Blackmore, J. Aldegunde, J. M. Hutson, and S. L. Cornish, Phys. Rev. A **96**, 021402 (2017).
[41] N. F. Ramsey, Phys. Rev. **78**, 695 (1950).
[42] A. P. Koller, J. Mundinger, M. L. Wall, and A. M. Rey, Phys. Rev. A **92**, 033608 (2015).
[43] A. Micheli, G. Pupillo, H. P. Büchler, and P. Zoller, Phys. Rev. A **76**, 043604 (2007).
[44] A. V. Gorshkov, S. R. Manmana, G. Chen, E. Demler, M. D. Lukin, and A. M. Rey, Phys. Rev. A **84**, 033619 (2011).
[45] M. P. Kwasigroch and N. R. Cooper, Phys. Rev. A **90**, 021605 (2014).